High Glucose and Glucosamine Induce Insulin Resistance via Different Mechanisms in 3T3-L1 Adipocytes

Bryce A. Nelson, Katherine A. Robinson, and Maria G. Buse

Sustained hyperglycemia induces insulin resistance, but the mechanism is still incompletely understood. Glucosamine (GlcN) has been extensively used to model the role of the hexosamine synthesis pathway (HSP) in glucose-induced insulin resistance. 3T3-L1 adipocytes were preincubated for 18 h in media ± 0.6 nmol/l insulin containing either low glucose (5 mmol/l), low glucose plus GlcN (0.1–2.5 mmol/l), or high glucose (25 mmol/l). Basal and acute insulin-stimulated (100 nmol/l) glucose transport was measured after re-equilibration in serum and insulin-free media. Preincubation with high glucose or GlcN (1–2.5 mmol/l) inhibited basal and acute insulin-stimulated glucose transport only if insulin was present during preincubation. However, only preincubation with GlcN plus insulin inhibited insulin-stimulated GLUT4 translocation. GLUT4 and GLUT1 protein expression were not affected. GlcN (2.5 mmol/l) increased cellular UDP-*N*-acetylhexosamines (UDP-HexNAc) by 400 and 900% without or with insulin, respectively. High glucose plus insulin increased UDP-HexNAc by 30%. GlcN depleted UDP-hexoses, whereas high glucose plus insulin increased them. Preincubation with 0.5 mmol/l GlcN plus insulin maximally increased UDP-HexNAc without affecting insulin-stimulated or basal glucose transport. GlcN plus insulin (but not high glucose plus insulin) caused marked GlcN dose-dependent accumulation of GlcN-6-phosphate, which correlated with insulin resistance of glucose transport (r = 0.935). GlcN plus insulin (but not high glucose plus insulin) decreased ATP (10–30%) and UTP (>50%). GTP was not measured, but GDP increased. Neither high glucose plus insulin nor GlcN plus insulin prevented acute insulin stimulation (~20-fold) of insulin receptor substrate 1–associated phosphatidylinositol (PI)-3 kinase. We have come to the following conclusions. *1*) Chronic exposure to high glucose or GlcN in the presence of low insulin caused insulin resistance of glucose transport by different mechanisms. *2*) GlcN inhibited GLUT4 translocation, whereas high glucose impaired GLUT4 "intrinsic activity" or membrane intercalation. *3*) Both agents may act distally to PI-3 kinase. *4*) GlcN has metabolic effects not shared by high glucose. GlcN may not model HSP appropriately, at least in 3T3-L1 adipocytes. *Diabetes* 49:981–991, 2000

Sustained hyperglycemia impairs insulin-stimulated glucose utilization by peripheral tissues (i.e., muscle and fat) in animal models and humans and decreases the ability of pancreatic β-cells to respond to hyperglycemia with acute insulin release. These observations gave rise to the "glucose toxicity" hypothesis, which is thought to account for the insulin resistance associated with uncontrolled type 1 diabetes and to contribute to insulin resistance in type 2 diabetes (1,2). Glucose transport is the rate-limiting step for glucose utilization by skeletal muscle and adipocytes under most conditions (1,3,4). In isolated rat adipocytes, chronic exposure to high glucose in the presence of insulin downregulates subsequent basal and acutely insulin-stimulated glucose transport; the effects of glucose and insulin during pre-exposure are synergistic (5) and appear to be associated with a post–insulin receptor defect (6).

Although the concept of glucose-induced insulin resistance is well documented, the underlying mechanisms are still not well understood. Marshall et al. (7) proposed that glucose-induced desensitization of glucose transport may be mediated by products of the hexosamine biosynthesis pathway (HSP). Glutamine:fructose-6-phosphate amidotransferase (GFAT) regulates the entry of glucose into this pathway by catalyzing the conversion of fructose-6-phosphate and glutamine to glucosamine-6-phosphate (GlcN-6-P) and glutamate. The major products of this pathway are UDP-*N*-acetylhexosamines (UDP-HexNAc), i.e., UDP-*N*-acetylglucosamine and UDP-*N*-acetylgalactosamine in an ~3:1 ratio (7). UDP-HexNAc are obligatory precursors for the synthesis of glycosyl side chains of proteins and lipids. Glucosamine (GlcN) enters cells on the same carrier as glucose, although its affinity for glucose transporters is less than that of glucose. On entry, GlcN is rapidly phosphorylated to GlcN-6-P. GlcN has been widely used as a model to assess the role of HSP products in insulin resistance (7–14). Because glucose-induced desensi-

From the Department of Medicine (B.A.N., K.A.R., M.G.B), Division of Endocrinology, Diabetes and Medical Genetics, and the Department of Biochemistry/Molecular Biology (M.G.B.), Medical University of South Carolina, Charleston, South Carolina.

Address correspondence and reprint requests to Maria G. Buse, MD, Medical University of South Carolina, Department of Medicine, Endocrinology, Diabetes and Medical Genetics Division, 96 Jonathan Lucas St., Suite 323, Charleston, SC 29425.

Received for publication 1 October 1999 and accepted in revised form 10 February 2000.

M.G.B. has received consulting fees from Monsanto (Searle).

2-DOG, 2-deoxy-D-glucose; 2-DOG-6-P, 2-deoxy-D-glucose-6-phosphate; 3-OMG, 3-*O*-methyl-D-glucose; ANOVA, analysis of variance; BSA, bovine serum albumin; DMEM, Dulbecco's minimal essential medium; FBS, fetal bovine serum; FITC-PE, fluorescein isothiocyanate–labeled phosphatidylethanolamine; GCV, GLUT4-containing vesicles; GFAT, glutamine:fructose-6-phosphate amidotransferase; GlcN, glucosamine; GlcN-6-P, glucosamine-6-phosphate; HPLC, high-pressure liquid chromatography; HSP, hexosamine biosynthetic pathway; IRS, insulin receptor substrate; KRBH, Krebs-Ringer bicarbonate/HEPES buffer; LDM, low-density microsomal; PBS, phosphate-buffered saline; PCA, perchloric acid; PI, phosphatidylinositol; PKB, protein kinase B; UDP-Hex, UDP-hexoses; UDP-HexNAc, UDP-*N*-acetylhexosamines.

tization requires several hours and primary cultures of skeletal muscle and adipocytes begin to dedifferentiate within 4–6 h, we used 3T3-L1 adipocytes as a model.

As reported in this article, we studied mechanisms by which glucose acts synergistically with insulin to desensitize the subsequent acute insulin response of glucose transport in 3T3-L1 adipocytes. We also compared the effects of high glucose to those of GlcN. Although both agents downregulated insulin-stimulated glucose transport, the mechanisms by which they achieved this were not identical.

RESEARCH DESIGN AND METHODS

Materials. Site-specific polyclonal rabbit antibodies against GLUT4 and GLUT1, respectively, were gifts from Dr. Mike Mueckler (Washington University, St. Louis, MO). A polyclonal antibody generated against the 14 COOH-terminal amino acids of rat liver insulin receptor substrate (IRS)-1 was purchased from Upstate Biotechnologies (Lake Placid, NY). Horseradish peroxidase–conjugated goat anti-rabbit IgG and rhodamine-conjugated antibodies were purchased from Jackson Immunoresearch Laboratories (West Grove, PA), and enhanced chemiluminescence reagents were purchased from Pierce (Rockford, IL). 2-[1,2-^{3}H]-deoxy-D-glucose, [^{3}H]-3-*O*-methylglucose, and [^{14}C]sucrose were bought from American Radiolabeled Chemicals (St. Louis, MO) and [γ-^{32}P]ATP from ICN Biomedicals (Costa Mesa, CA). Bovine serum albumin (BSA) and crystalline BSA were bought from Intergen (Purchase, NY) and Calbiochem (La Jolla, CA), respectively. Fluorescein isothiocyanate–labeled phosphatidylethanolamine (FITC-PE), phosphatidylinositol (PI), and PI-4 phosphate were from Avanti Polar Lipids (Alabaster, AL). Tissue culture reagents were purchased from Gibco (Grand Island, NY), with the exception of fetal bovine serum (FBS) and calf serum, which were bought from Biofluids (Rockville, MD). COOH-terminal GLUT1 and GLUT4 peptides were prepared by the peptide synthesis facility at the Medical University of South Carolina. Other reagents were purchased from Fisher or Sigma or from suppliers identified in previous publications (14–18).

Cell culture and general methods. 3T3-L1 fibroblasts were grown and differentiated into adipocytes in 35-mm culture dishes, as described by Frost and Lane (19). Cells were grown to confluence in Dulbecco's minimal essential medium (DMEM) containing 25 mmol/l glucose and 10% calf serum at 37°C in a humidified atmosphere containing 5% CO_2. Two days after confluence, cells were placed in DMEM containing 25 mmol/l glucose, 0.5 mmol/l isobutylmethylxanthine, 1 µmol/l dexamethasone, 10 µg/ml insulin, and 10% FBS for 3 days and then for 2 days in DMEM containing 25 mmol/l glucose, 10 µg/ml insulin, and 10% FBS. Thereafter, cells were maintained in and refed every 2 days with DMEM, 25 mmol/l glucose, and 10% FBS until used in experiments 10–14 days after the start of treatment, when between 90 and 95% of the cells exhibited adipocyte phenotype.

In typical experiments, 3T3-L1 adipocytes were preincubated for 18 h at 37°C with DMEM (1% FBS) containing 5 mmol/l glucose with or without 0.6 nmol/l insulin, 5 mmol/l glucose plus 2.5 mmol/l GlcN with or without 0.6 nmol/l insulin, or 25 mmol/l glucose with or without 0.6 nmol/l insulin. The insulin concentration in the media was determined by radioimmunoassay at the start of preincubation. There was 1 nmol/l insulin added to the media, but ~40% was lost during filter sterilization and by adsorption to plastic ware. At the end of the preincubation, insulin concentrations had decreased to ~0.3 nmol/l, reflecting insulin degradation by the cells (20).

Media glucose concentration decreased minimally when cells were preincubated in either medium in the absence of insulin. When insulin was included in the media, glucose concentrations decreased significantly by 86% (low glucose, 5.17 ± 0.18 vs. 0.72 ± 0.02, $P < 0.001$), 85% (low glucose plus GlcN, 5.62 ± 0.07 vs. 0.845 ± 0.07, $P < 0.05$), and 43% (high glucose, 26.31 ± 0.99 vs. 14.98 ± 1.12, $P < 0.001$) after 18 h.

After preincubation, adipocytes were washed 3 times with phosphate-buffered saline (PBS) containing 0.1% BSA at 37°C and incubated for 2 h in serum- and insulin-free DMEM containing the same sugar concentrations that were added to the preincubation media with 0.5% BSA and 25 mmol/l HEPES at 37°C in a 5% CO_2 atmosphere. Cells were then rapidly washed 3 times and equilibrated for 10 min at 37°C with 0.1% BSA in Krebs-Ringer bicarbonate/HEPES buffer (KRBH), pH 7.4 (KRBH = 25 mmol/l HEPES, 120 mmol/l NaCl, 4.6 mmol/l KCl, 1.9 mmol/l $CaCl_2$, 1 mmol/l $MgSO_4$, and 1.2 mmol/l KH_2PO_4).

Glucose transport. Cells prepared as described above were incubated in glucose-free KRBH at 37°C with or without an acute insulin dose (100 nmol/l) for 15 min. Glucose transport was initiated by the addition of 2-deoxy-D-glucose (2-DOG) (0.05 mmol/l and 0.5 µCi/ml). [^{14}C]sucrose (0.05 mmol/l and 0.05 µCi/ml) was also added as an extracellular space marker. After 5 min at 37°C, 2-DOG transport was terminated by the addition of phloretin (48 µmol/l). The cells were immediately placed on ice and washed 3 times with ice-cold PBS and solubilized with 1% Triton X-100. ^{3}H and ^{14}C concentrations were determined by liquid scintillation spectrometry. The intracellular concentration of 2-DOG was calculated by correcting for the label present in the extracellular space and normalized to the protein concentration in the extract.

In additional experiments, 3-*O*-methyl-D-glucose (3-OMG) transport was measured as described by Sweeney et al. (21). Briefly, cells were washed and equilibrated for 10 min at 37°C with HEPES-buffered saline (140 mmol/l NaCl, 20 mmol/l HEPES, pH 7.4, 2.5 mmol/l $MgSO_4$, 1 mmol/l $CaCl_2$, and 5 mmol/l KCl) and then acutely stimulated with or without insulin (100 nmol/l) for 15 min. The buffer was aspirated, and cells were exposed for 30 s to HEPES-buffered saline containing 50 µmol/l 3-*O*-[^{3}H]-methylglucose (4 µCi/ml) and 50 µmol/l [^{14}C]sucrose (0.4 µCi/ml). The cells were then immediately placed on ice, washed 3 times with 1 mmol/l $HgCl_2$ in saline, and lysed with 0.05 N NaOH, and ^{3}H and ^{14}C concentrations were determined by liquid scintillation spectrometry.

Glucose transporter expression. For GLUT4 detection by Western blot, 30 µg total cell protein from the lysates prepared during the 2-DOG transport assay was separated by Laemmli's SDS-PAGE. To detect GLUT1, in separate experiments, total membrane fractions were prepared by homogenizing cells in buffer containing 0.25 mol/l sucrose, 10 mmol/l Tris, pH 7.4, 2 mmol/l EDTA, and protease inhibitors. The homogenate was centrifuged for 5 min at 1,000 rpm in a tabletop centrifuge, and the fat layer was removed. The aqueous infranatant was then centrifuged at 4°C for 2 h at 200,000*g*. The resulting pellet was resuspended in the same buffer supplemented with 1% Triton X-100. After 30 min at 4°C, the suspension was centrifuged for 10 min at 10,000*g*, and 10 µg protein from the supernatant was analyzed by Laemmli's SDS-PAGE. After separation, proteins were transferred to nitrocellulose membranes, blocked with 5% dry nonfat milk/Tris-buffered saline for 1 h, immunoblotted at 4°C overnight with rabbit α-GLUT4 (1:500) or rabbit α-GLUT1 (1:500) IgG, detected with horseradish peroxidase–conjugated goat anti-rabbit IgG (1:10,000) and enhanced chemiluminescence, and scanned by laser densitometry as previously described (18). Bands were quantitated using NIH Image 1.61 software (www.nih.gov).

GLUT4 translocation. Cells prepared as above were stimulated with or without insulin (100 nmol/l) for 15 min. Dish-adherent plasma membrane sheets were prepared by a modification of described protocols (22–24). Briefly, cells were placed on ice and washed twice in ice-cold buffer A (50 mmol/l HEPES, pH 7.2, and 100 mmol/l NaCl) and once in ice-cold buffer B (20 mmol/l HEPES, pH 7.2, 100 mmol/l KCl, 2 mmol/l $CaCl_2$, 1 mmol/l $MgCl_2$, 2 µg/ml trypsin inhibitor, 10 µmol/l leupeptin, and 0.5 mmol/l benzamidine). The cells were then ruptured by mechanical shearing with a controlled stream of buffer B, washed twice with buffer B, and fixed for 15 min with 3.7% paraformaldehyde/PBS. Membrane sheets were then washed 3 times with PBS and stained with 10 µg/ml FITC-PE for 15 min, washed 3 times with PBS, blocked for 10 min with 0.2% crystalline BSA/PBS, and after 3 more PBS washes, immunostained with rabbit α-GLUT4 IgG (1:100 in 0.2% crystalline BSA/PBS) for 30 min. After 3 PBS washes and blocking, plates were incubated for 30 min with rhodamine-conjugated goat anti-rabbit IgG (1:40), and after further washing and blocking, they were incubated for 30 min with rhodamine-conjugated rabbit anti-goat IgG. After 3 washes with PBS, plates were postfixed with 3.7% formaldehyde and coverslipped.

To quantitate plasma membrane–associated GLUT4, plates were coded before immunostaining to blind the investigator to the treatment conditions and to prevent bias during quantitation and image acquisition. Three digital images per plate were acquired using a Zeiss Axioplan microscope (Zeiss, Jena, Germany) equipped with a DAGE 100 integrating charge-coupled device camera and NIH Image software. Fields were picked based solely on their FITC-PE labeling (green fluorescence) with no data on their corresponding red fluorescence (rhodamine labeling). Eight membrane sheets per image were quantitated as mean pixel brightness using NIH Image 1.61 software. Three measurements of background mean pixel brightness were taken in areas lacking membrane remnants and subtracted. In some experiments, plates were stained only with the rhodamine-conjugated antibodies and not incubated with α-GLUT4 to quantitate nonspecific binding of the secondary and tertiary antibodies. This value typically represented 8–10% of the total mean pixel brightness and was subtracted from each data point. As an additional control for the specificity of immunostaining, some plates were initially immunostained with rabbit α-GLUT4 IgG in the presence of the 15-mer COOH-terminal peptide (10 µg/ml) to which the antibody was generated (25).

Analysis of nucleotide-linked hexoses and hexosamines. This procedure and its validation have been described in detail (15–17). After 18 h of preincubation in conditions described in CELL CULTURE AND GENERAL METHODS, 35-mm plates of 3T3-L1 adipocytes were washed once with ice-cold PBS and quick-frozen in liquid N_2. Cells were homogenized in 0.5 ml of 0.3 mol/l perchloric acid (PCA) with a Potter-Elvehjem homogenizer. The precipitates were pelleted

by centrifugation (5 min, 10,000*g*, 4°C), and PCA was extracted from the supernatants with 2 volumes of 1:4 trioctylamine:1,1,2 trichloro-fluoroethane (Freon). The aqueous phase was stored at –80°C and analyzed within 5 days. Nucleotide-linked hexoses and hexosamines were separated and measured by anion exchange high-pressure liquid chromatography (HPLC). UDP-HexNAc, UDP-hexoses (UDP-Hex), GDP mannose, and UDP were quantified by ultraviolet absorption (A_{254}) and compared with external standards.

Nucleotide analysis. Deproteinized cell extracts were prepared as described above and stored at –80°C for <24 h before HPLC analysis. Nucleotides were separated on a Beckman Ultrasphere ODS 5 µm C_{18} reverse-phase HPLC column (Beckman, Fullerton, CA) eluted isocratically with 100 mmol/l triethylamine phosphate, pH 5.8/1% acetonitrile, as previously described (17). ATP, ADP, GDP, and UTP were quantitated by ultraviolet absorption and compared with external standards. GTP coeluted with an unidentified compound in this system and was not quantifiable. The ultraviolet absorbing compound may be fat cell specific because GTP was easily separated in muscle extracts using the same method (17).

Analysis of GlcN-6-P concentration. Aliquots (100 µl) of PCA extracts were derivatized with *o*-phthaldialdehyde (8 mg/ml), and GlcN-6-P concentration was quantified fluorometrically by reverse-phase HPLC as previously described (15–17). The lower limit of detection by this method is ~40 pmol.

Assay of PI-3 kinase activity. Cells grown on 60-mm plates were prepared, preincubated for 18 h under conditions indicated in RESULTS, and serum-starved for 2 h as described in CELL CULTURE AND GENERAL METHODS. PI-3 kinase activity was measured essentially as described by Kelly et al. (26), with some modification. After a 10-min equilibration in 0.1% BSA/KRBH, cells were incubated with or without 100 nmol/l insulin for 5 min, washed twice with ice-cold PBS, quick-frozen in liquid N_2, and homogenized with a Potter-Elvehjem homogenizer in buffer containing 50 mmol/l HEPES, pH 7.5, 10 mmol/l EDTA, 100 mmol/l NaF, 40 mmol/l NaCl, 10 mmol/l sodium pyrophosphate, 0.2 mmol/l Na_3VO_4, 10% glycerol, 1 mmol/l phenylmethylsulfonyl fluoride, and 0.1 mg/ml aprotinin. The samples were then centrifuged for 1 min at 10,000*g*; the infranatant was removed and centrifuged at 10,000*g* for 1 min. The fat-free supernatant was supplemented with 1% NP-40 detergent, placed on ice, and then centrifuged for 10 min at 10,000*g*. An aliquot of the supernatant (200 µg protein) was incubated overnight with α–IRS-1 IgG (2 µg) and then with 40 µl of a 50% slurry of protein A sepharose at 4°C for 2 h. The immunoprecipitates were pelleted at 2,500*g* for 10 s at room temperature and washed twice with PBS, pH 7.4, 0.1 mmol/l Na_3VO_4, and 1% NP-40; twice with 0.5 mmol/l LiCl, 100 mmol/l Tris, pH 7.4, and 0.1 mmol/l Na_3VO_4; and twice with assay buffer (10 mmol/l Tris, pH 7.4, 100 mmol/l NaCl, 1 mmol/l EDTA, 0.1 mmol/l Na_3VO_4, and 10 mmol/l $MgCl_2$), and were then resuspended in an emulsion of assay buffer containing PI (0.22 µg/µl, prepared by sonication). The reaction was initiated by adding [γ-^{32}P]ATP (0.04 mmol/l and 30 µCi/sample) and after 20 min at room temperature was stopped with HCl (1.3 mol/l final concentration). Lipids were extracted into 1 volume of chloroform:methanol (1:1), centrifuged for 5 min at 2,500*g*, and separated on thin-layer chromotagraphy plates (Whatman, Clifton, NJ) in a solvent containing chloroform:methanol:water:ammonium hydroxide (60:47:11.3:2, vol/vol). The plates were air-dried and developed by autoradiography. Spots were scraped and counted by liquid scintillation spectrometry. The spots' R_f was compared with both a PI and a PI-4-phosphate standard, which were visualized by ammonium molybdate staining as described previously (26).

Other analyses. Insulin concentration in the media was determined by radioimmunoassay (Linco Research, St. Charles, MO). Media glucose concentration was measured by the glucose oxidase method using a Beckman Glucose Analyzer II (Beckman). Protein concentrations in cell extracts were measured spectrophotometrically against BSA standards using Coomassie protein assay reagent purchased from Pierce (Rockford, IL).

Statistical analysis. Means ± SE are shown. Error bars are not indicated in the figures if they are too small for graphical representation, i.e., they fall within the symbol of the mean. The significance of differences between means was evaluated by 1-way or 2-way analysis of variance and Tukey's test for unbalanced design using the Statistica software (Tulsa, OK) or by 2-tailed unpaired Student's *t* test using Statview software (Abacus Concepts, Berkeley, CA). $P < 0.05$ was considered significant.

RESULTS

Glucose transport. As expected after differentiation, 3T3-L1 adipocytes exhibited a marked response to an acute maximal dose of insulin (100 nmol/l) with significant ($P < 0.001$) increases in glucose transport above basal under all conditions studied. When cells were preincubated for 18 h in media containing 5 mmol/l glucose, acute maximal insulin stimulation (100 nmol/l) induced an ~4-fold increase in 2-DOG transport (Fig. 1*A*). The addition of 0.6 nmol/l insulin during preincubation did not significantly affect either basal or insulin-stimulated 2-DOG transport. Also, when cells were preincubated without insulin in either 5 mmol/l glucose plus 2.5 mmol/l GlcN or 25 mmol/l glucose, the acute maximal insulin response of glucose transport was not significantly different when compared with cells preincubated in 5 mmol/l glucose. On the other hand, 18 h of preincubation in media containing GlcN or high glucose in the presence of 0.6 nmol/l insulin decreased acute maximal insulin-stimulated glucose transport by 43 and 42%, respectively (Fig. 1*A*, $P < 0.001$), when compared with cells preincubated with 5 mmol/l glucose in the presence of 0.6 nmol/l insulin. Basal or insulin-independent glucose transport also decreased by 36 and 46%,

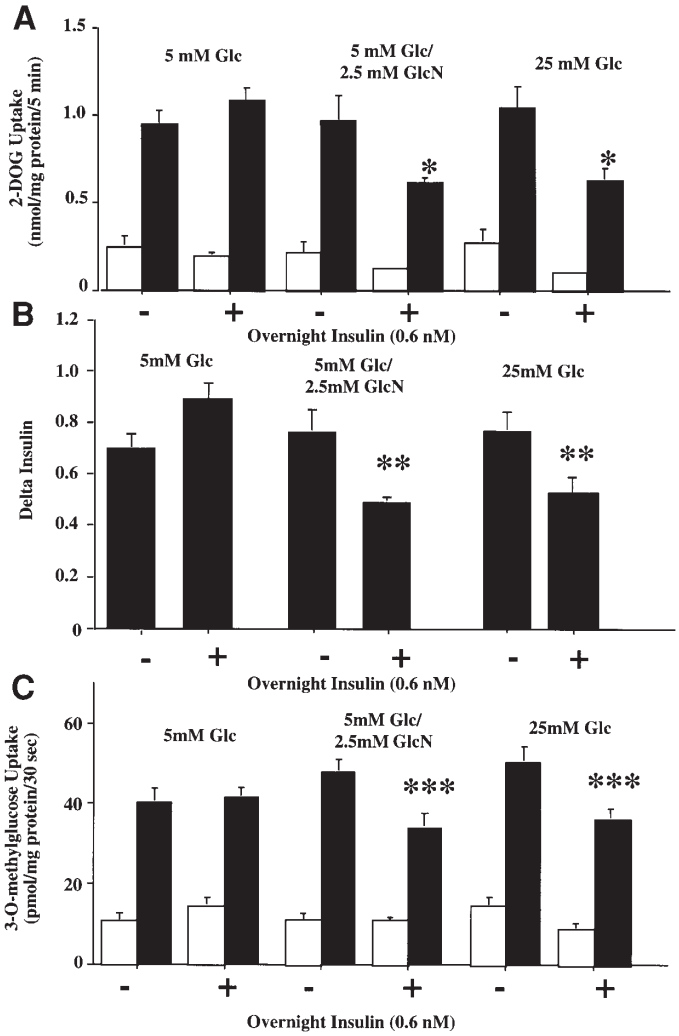

FIG. 1. Glucose transport in 3T3-L1 adipocytes. After an 18-h preincubation in media containing either 5 mmol/l glucose (Glc) with or without 0.6 nmol/l insulin, 5 mmol/l glucose plus 2.5 mmol/l GlcN with or without 0.6 nmol/l insulin, or 25 mmol/l glucose with or without 0.6 nmol/l insulin, cells were washed, equilibrated in glucose-free KRBH containing 0.1% BSA, and acutely stimulated with (■) or without (□) 100 nmol/l insulin for 15 min. *A*: 2-DOG uptake was measured over 5 min and normalized to protein concentrations as described in RESEARCH DESIGN AND METHODS. *B*: Delta insulin was calculated as the absolute difference between basal and acute insulin-stimulated 2-DOG transport after each preincubation. *C*: 3-OMG transport was measured after 30 s as described in RESEARCH DESIGN AND METHODS. Data bars represent the means ± SE from 5 (*A* and *B*) or 3 (*C*) experiments performed in duplicate. *$P < 0.001$; **$P < 0.006$; ***$P < 0.05$.

respectively, after preincubation with GlcN or high glucose in the presence of 0.6 nmol/l insulin for 18 h, although differences did not reach statistical significance. Acute insulin-stimulated 2-DOG transport above basal (Δ insulin) also decreased by ~40% after preincubation with GlcN or high glucose in the presence of 0.6 nmol/l insulin as compared with the control (Fig. 1*B*, $P < 0.006$). Thus, the decrease in the acute maximal insulin response is not accounted for solely by a decrease in basal 2-DOG transport. The induction of this desensitization required at least 6 h and was maximal by 18 h (data not shown).

2-DOG is transported into cells in the same way as glucose; on entry, it is phosphorylated to 2-deoxy-D-glucose-6-phosphate (2-DOG-6-P), which is not further metabolized and is trapped intracellularly. To assess whether the downregulation of insulin-stimulated 2-DOG uptake after pre-exposure to high glucose or GlcN in the presence of insulin reflected effects on sugar transport or phosphorylation, in some experiments, we measured 3-OMG transport. The latter is transported like glucose into cells but is not phosphorylated. The data are similar to those obtained in 2-DOG uptake studies (Fig. 1*C*). Preincubation in the presence of 0.6 nmol/l insulin decreased subsequent acute insulin-stimulated 3-OMG transport (vs. cells preincubated without insulin) if high glucose ($P < 0.001$) or GlcN ($P < 0.05$) was present during preincubation but not if low glucose was present. We concluded that insulin is required for glucose- and GlcN-induced desensitization of acute insulin-stimulated glucose transport and that both high-glucose and GlcN pretreatment affect glucose transport per se.

Glucose transporter expression. The decrease in insulin-stimulated glucose transport could be explained by decreased expression of the glucose transporter isoforms GLUT1 and/or GLUT4. It has been previously suggested that in this cell type, insulin resistance is associated with decreased GLUT4 expression (20). A representative immunoblot is shown in Fig. 2*A*, and the densitometric quantitation of the means from 5 independent experiments are shown in Fig. 2*B*. Total GLUT4 protein levels were determined in parallel with glucose transport using the same cell lysates. After an 18-h preincubation in media containing either high glucose (25 mmol/l glucose) or GlcN (5 mmol/l glucose plus 2.5 mmol/l GlcN), total GLUT4 protein levels were not significantly different from cells preincubated in media containing 5 mmol/l glucose. Further, the addition of insulin during preincubation did not significantly alter total GLUT4 expression. Similar results were obtained when GLUT4 expression was quantitated in total membrane preparations (data not shown). The latter preparation was used to quantitate GLUT1 expression, and again, no significant differences were detected between the treatment conditions (Fig. 2*C* and *D*).

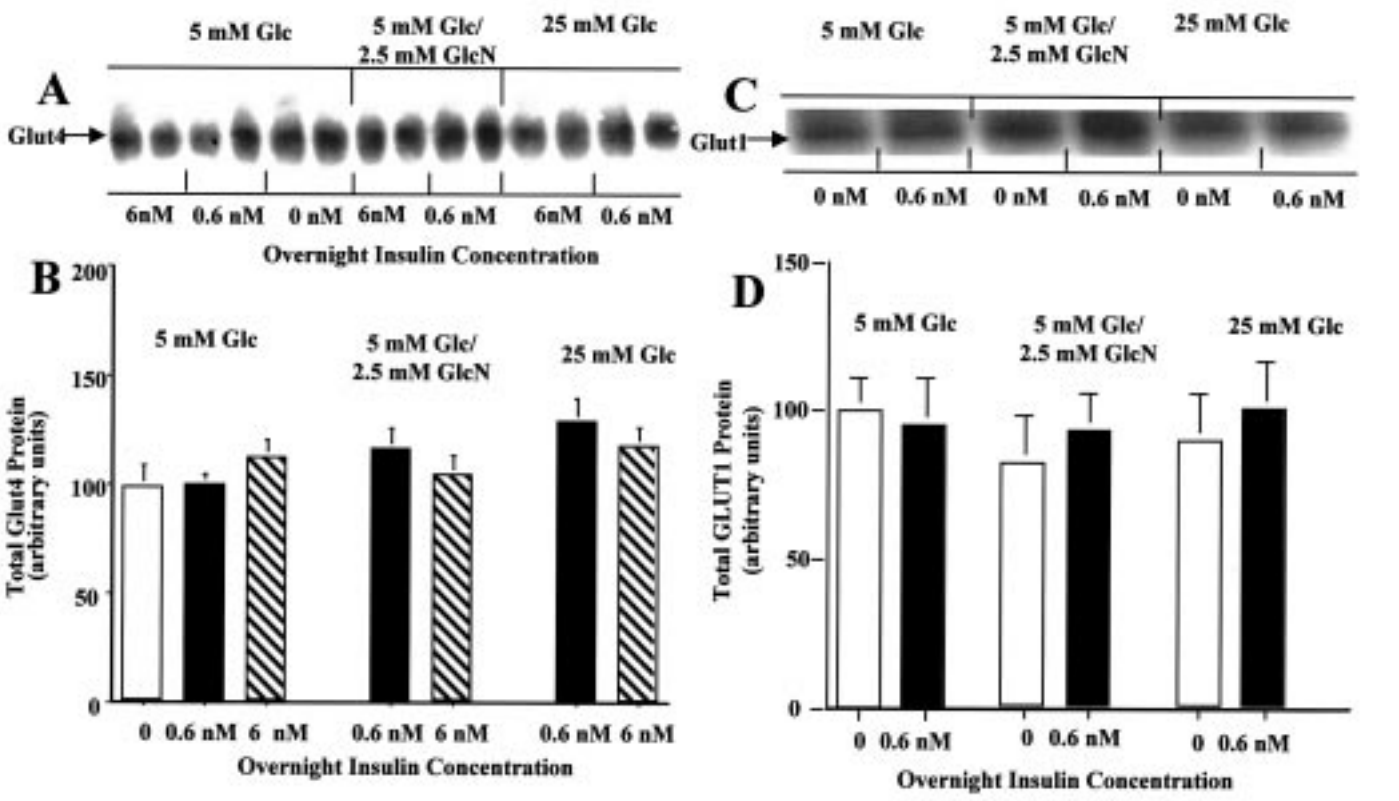

FIG. 2. GLUT4 and GLUT1 protein expression. Total GLUT4 protein levels were determined in parallel with glucose (Glc) transport from 1% Triton X-100 solubilized total cell extracts. *A*: Representative immunoblot of 30 µg total cell protein separated by Laemmli's SDS-PAGE and immunoblotted with polyclonal rabbit α-GLUT4. *B*: Densitometric analysis of GLUT4 immunoblots from 5 independent experiments. Data are normalized to GLUT4 levels after preincubation with 5 mmol/l glucose plus 0.6 nmol/l insulin, each analyzed in duplicate or quadruplicate. *C* and *D*: Representative immunoblot for GLUT1 using 10 µg total membrane protein prepared as described in RESEARCH DESIGN AND METHODS and the subsequent densitometric analysis of 3 independent experiments.

GLUT4 translocation. We next assessed whether the decrease in insulin-stimulated glucose transport was associated with a defect in insulin-induced recruitment of GLUT4 to the plasma membrane. Plasma membrane lawns were prepared as described in RESEARCH DESIGN AND METHODS after a 15-min stimulation with or without 100 nmol/l insulin. An acute maximal insulin dose markedly increased plasma membrane–associated GLUT4 immunostaining after all preincubation conditions (Fig. 3*A*). However, insulin-stimulated GLUT4 translocation to the plasma membrane was impaired by ~45% ($P < 0.0007$) only in those cells preincubated with GlcN plus insulin but not in the cells preincubated with high glucose plus insulin (Fig. 3*B*). Neither high glucose nor GlcN affected GLUT4 translocation in the absence of insulin during preincubation. Basal association of GLUT4 with the plasma membrane was not affected significantly by any of the preincubation conditions. These data suggest that in the presence of insulin, high glucose and GlcN act via different mechanisms in downregulating glucose transport.

Nucleotide sugars. To assess the contribution of HSP to glucose transport desensitization, nucleotide sugar concentrations in the cells were measured. UDP-HexNAc (which represents both UDP-*N*-acetylglucosamine and UDP-*N*-acetylgalactosamine in an ~3:1 ratio) is the major product of HSP. Preincubation with low glucose plus insulin had no significant effect on UDP-HexNAc concentration (100% = 6.76 ± 0.659 nmol UDP-HexNAc/mg protein) as compared with its concentration after preincubation with low glucose in the absence of insulin (Fig. 4*A*).

As expected, preincubation with GlcN markedly increased UDP-HexNAc concentration as compared with control (low glucose plus insulin) by ~400 and ~900% in the absence and presence of insulin, respectively (Fig. 4*A*, $P < 0.0005$). Preincubation with high glucose, on the other hand, increased UDP-HexNAc concentration only modestly by ~30%. This increase required the presence of insulin and was significant ($P < 0.001$) compared with low glucose plus insulin.

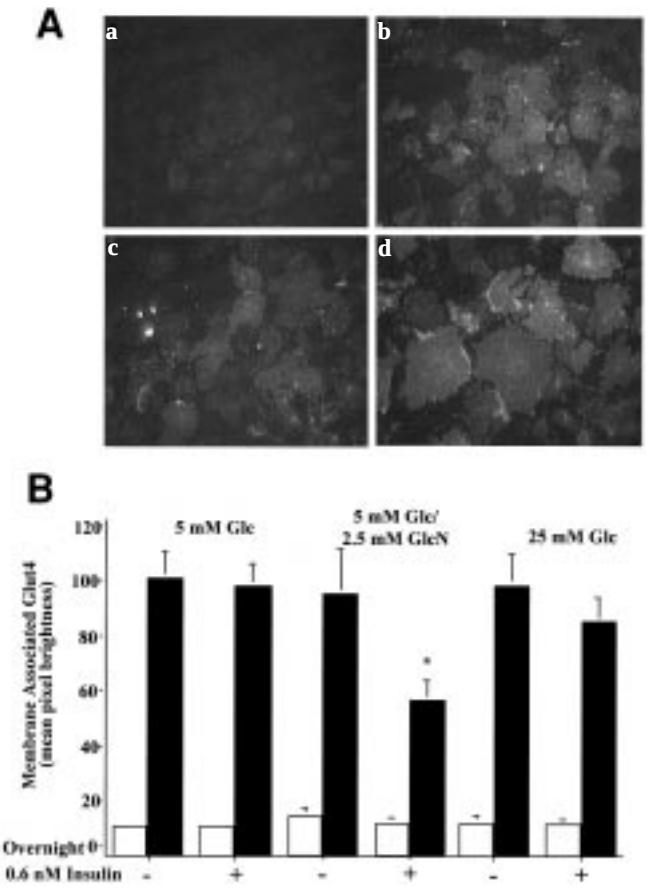

FIG. 3. GLUT4 translocation. Cells were preincubated for 18 h as described in Fig. 1, and plasma membrane remnants were prepared as described in RESEARCH DESIGN AND METHODS. *A*: Black and white images of GLUT4 immunofluorescence after acute stimulation without (a) or with (b, c, and d) 100 nmol/l insulin after preincubation with either 5 mmol/l glucose (Glc) plus insulin (a and b) or 5 mmol/l glucose plus 2.5 mmol/l GlcN plus 0.6 nmol/l insulin (c) or 25 mmol/l glucose plus 0.6 nmol/l insulin (d). *B*: The quantitation of GLUT4 plasma membrane immunofluorescence (mean pixel brightness) after acute 15-min stimulation without (□) or with (■) 100 nmol/l insulin after preincubation under the conditions indicated. Data are normalized to those observed in cells preincubated with 5 mmol/l glucose plus 0.6 nmol/l insulin and then acutely stimulated with 100 nmol/l insulin. Each bar represents the means ± SE of 3–5 experiments performed in duplicate. *$P < 0.0007$.

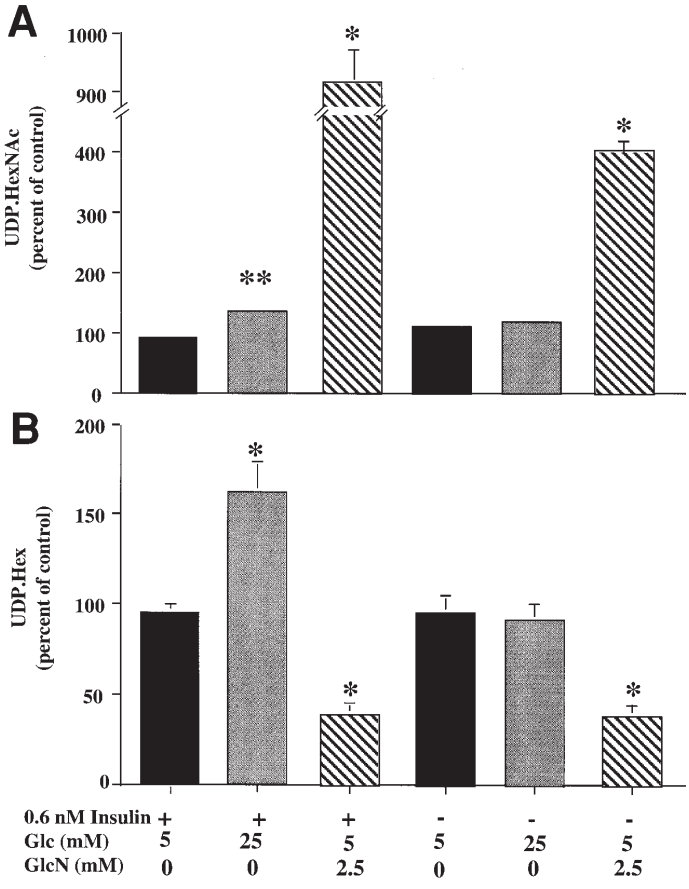

FIG. 4. UDP-HexNAc and UDP-Hex concentration. UDP-HexNAc (*A*) and UDP-Hex (*B*) were analyzed by anion-exchange HPLC from PCA extracts of 3T3-L1 adipocytes after preincubation with either 5 mmol/l glucose (Glc) with or without 0.6 nmol/l insulin (■), 5 mmol/l glucose plus 2.5 mmol/l GlcN with or without 0.6 nmol/l insulin (▨), or 25 mmol/l glucose with or without 0.6 nmol/l insulin (▩) and normalized to cells preincubated with 5 mmol/l glucose plus 0.6 nmol/l insulin (UDP-HexNAc, 100% = 6.76 ± 0.659 nmol/mg protein; UDP-Hex, 100% = 3.221 ± 0.490 nmol/mg protein). Bars represent means ± SE of at least 3 experiments performed in duplicate. *$P < 0.001$; **$P < 0.01$.

The measurement of UDP-Hex (Fig. 4*B*) represents the concentrations of UDP-glucose plus UDP-galactose in an ~3:1 ratio. UDP-glucose is the obligatory substrate of glycogen synthase. Preincubation with GlcN or high glucose exerted opposing effects on cellular UDP-Hex concentrations. High glucose in the presence of insulin, but not in its absence, increased cellular UDP-Hex concentrations by ~60% ($P < 0.01$, compared with preincubation in 5 mmol/l glucose). In contrast, preincubation with 2.5 mmol/l GlcN in the presence of 5 mmol/l glucose depleted UDP-Hex concentrations by ~60% in the presence or absence of insulin ($P < 0.01$).

The data in Figs. 1*A* and 4*A* suggest that there is no simple correlation between cellular concentrations of UDP-HexNAc and the development of insulin-resistant glucose transport. Preincubation in 2.5 mmol/l GlcN in the absence of insulin increased intracellular UDP-HexNAc ~4-fold but failed to cause insulin resistance. Preincubation with low-dose insulin in the presence of high glucose or GlcN caused similar (~45%) inhibition of the insulin response, yet UDP-HexNAc increased by 900% in the latter condition and by only 30% in the former condition.

To further analyze the relationship between the accumulation of UDP-HexNAc and the impairment of basal and maximal insulin-stimulated 2-DOG transport, cells were preincubated for 18 h in 5 mmol/l glucose plus 0.6 nmol/l insulin with or without varying concentrations of added GlcN (0.1–2.5 mmol/l, Fig. 5). In the presence of insulin, cellular UDP-HexNAc concentrations rose steeply and dose dependently between 0.1 and 0.5 mmol/l GlcN and were increased ~10-fold at 0.5 mmol/l GlcN. No further increase in UDP-HexNAc was observed between 0.5 and 2.5 mmol/l GlcN, and levels tended to fall (Fig. 5*A*). Under the same conditions, maximal insulin-stimulated 2-DOG transport or basal 2-DOG transport were not inhibited after preincubation with 0.5 mmol/l GlcN but decreased between 1 and 2.5 mmol/l GlcN. Maximal inhibition at 2.5 mmol/l GlcN was ~50% for insulin-stimulated transport ($P < 0.01$) and ~30% for basal transport (Fig. 5*B*). Insulin-mediated GLUT4 translocation also decreased in parallel to 2-DOG transport after preincubation with increasing concentrations of GlcN in the presence of insulin (Fig. 5*C*). These data suggest that in the presence of insulin, the maximal capacity of these cells to metabolize GlcN to UDP-HexNAc is reached at ~0.5 mmol/l GlcN in the medium. Furthermore, there appears to be no correlation between cellular UDP-HexNAc accumulation and the development of insulin-resistant glucose transport in this model.

Nucleotide concentrations. The data suggested that UTP availability may limit the formation of UDP-Hex (Fig. 4*B*) and UDP-HexNAc (Fig. 5*A*) in cells preincubated with increasing doses of GlcN both in the presence or absence of insulin. Furthermore, Hresko et al. (27) recently reported that ATP depletion may account for the development of GlcN-induced insulin resistance in 3T3-L1 adipocytes. We therefore measured the concentration of several nucleotides in 3T3-L1 adipocytes incubated for 18 h in media with or without 0.6 nmol/l insulin and containing 5 mmol/l glucose, 5 mmol/l glucose supplemented with increasing concentrations of GlcN (0.1–2.5 mmol/l), or 25 mmol/l glucose. As shown in Fig. 6, ATP did not change significantly in the presence of increasing concentrations of GlcN without insulin. In the presence of insulin, ATP tended to decline 10–20% at low GlcN concentrations (0.1–0.5 mmol/l) and 25–30% after incubation with 1–2.5 mmol/l GlcN ($P < 0.0002$). ADP tended to increase with increasing concentrations of GlcN, but the effect did not reach statistical significance. GDP concentrations were elevated with increasing concentrations of GlcN by more than ~50%; the GlcN effect was statistically significant only in the presence of insulin ($P < 0.0002$). UTP concentrations decreased significantly during incubation with GlcN with or without insulin ($P < 0.0001$). The lowest concentration of GlcN tested (0.1 mmol/l) decreased UTP by ~30%, and depletion was near maximal at 1 mmol/l GlcN.

The effects on nucleotide concentrations of incubation in low glucose versus high glucose in the absence and presence of insulin are shown in Fig. 7. Insulin did not affect ATP or ADP concentrations during incubation in low glucose. High glucose tended to increase the concentration of ATP (vs. low glucose), but the effect was only significant in the absence of insulin ($P < 0.05$) by 1-way analysis of variance (ANOVA). Changes in ADP concentration paralleled those in ATP ($P < 0.05$). The ratio of ATP to ADP was unchanged (~10) in each condition. By 2-way ANOVA, high glucose but not insulin increased both ATP

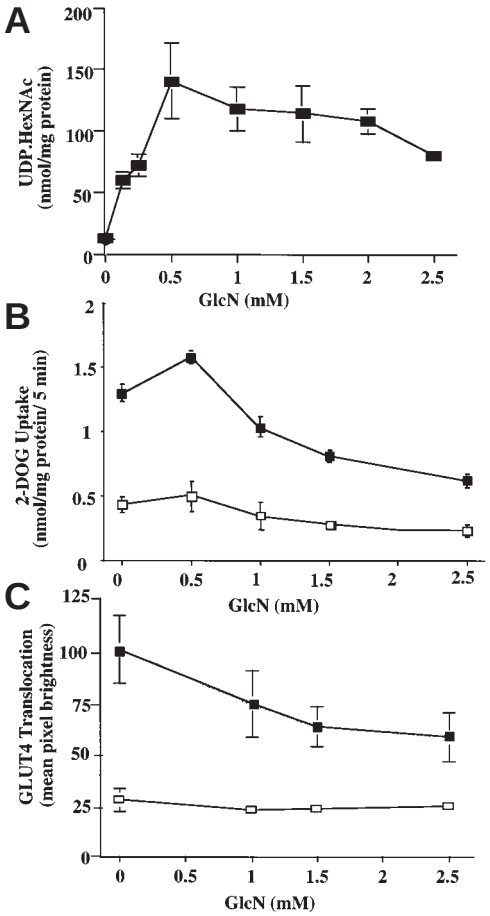

FIG. 5. GlcN dose response of UDP-HexNAc accumulation, 2-DOG transport, and GLUT4 plasma membrane association. Cells were preincubated as described in media containing 5 mmol/l glucose plus 0.6 nmol/l insulin supplemented with increasing concentrations of GlcN (0.1–2.5 mmol/l). *A*: UDP-HexNAc levels were measured as in Fig. 4. 2-DOG transport (*B*) and GLUT4 translocation (*C*) were measured as described in Figs. 1 and 3, respectively, after a 15-min acute stimulation without (□) or with (■) 100 nmol/l insulin. Data are means ± SE of at least 3 experiments performed in duplicate.

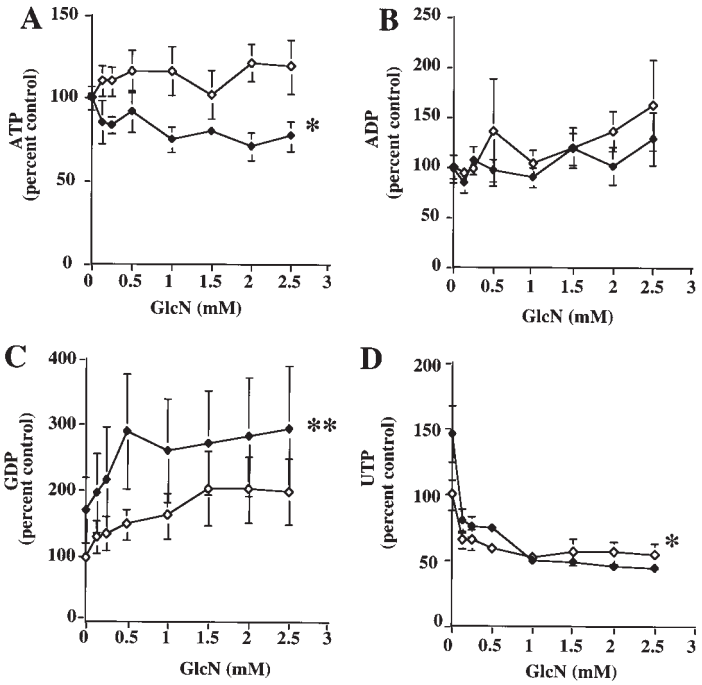

FIG. 6. GlcN effect on nucleotide concentrations. After an 18-h preincubation with 5 mmol/l glucose without (◇) or with (◆) 0.6 nmol/l insulin with increasing concentrations of GlcN (0–2.5 mmol/l), PCA extracts were prepared and neutralized, and ATP (*A*), ADP (*B*), GDP (*C*), and UTP (*D*) were separated by reverse-phase HPLC. Data are normalized to values measured in cells preincubated in media containing 5 mmol/l glucose without GlcN or insulin. 100% = 25.83 ± 5.50 nmol/mg protein for ATP, 2.46 ± 0.32 for ADP, 1.08 ± 0.15 for GDP, and 5.17 ± 1.06 for UTP. Data points represent means ± SE from 3 experiments performed in duplicate. *$P < 0.0002$; **$P < 0.0001$.

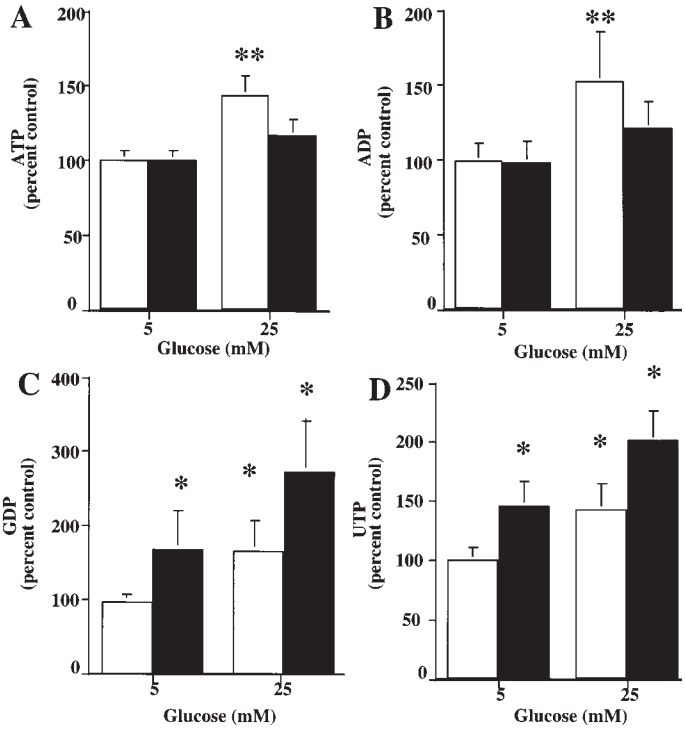

FIG. 7. Glucose and insulin effect on nucleotide concentrations. Cells were preincubated with either 5 or 25 mmol/l glucose in the absence (□) or presence (■) of 0.6 nmol/l insulin, and PCA extracts were prepared. ATP (*A*), ADP (*B*), GDP (*C*), and UTP (*D*) were separated by reverse-phase HPLC. Data are normalized to values observed after preincubation with media containing 5 mmol/l glucose without insulin. Absolute values are indicated in the legend of Fig. 6. Data points represent means ± SE from 3 experiments performed in duplicate. *By 2-way ANOVA, both insulin and high glucose independently increased GDP and UTP ($P < 0.01$); **$P < 0.05$ vs. low glucose.

($P < 0.0003$) and ADP ($P < 0.01$) concentrations, whereas both high glucose and insulin appeared to independently increase the concentrations of GDP ($P < 0.01$) and UTP ($P < 0.006$).

GlcN-6-P. If the rate-limiting step in the metabolism of GlcN to UDP-HexNAc is distal to hexokinase, intracellular GlcN-6-P may accumulate with increasing GlcN concentrations in the medium. The latter may explain the observed depletion of ATP. GlcN-6-P was undetectable in the cells (the lower limit of detection using this method is ~40 pmol) after preincubation with low glucose or high glucose with or without insulin (data not shown). GlcN-6-P was only minimally elevated with increasing concentrations of GlcN (0.1–2.5 mmol/l) in the absence of insulin increasing to 0.44 ± 0.05 nmol/mg protein with 2.5 mmol/l GlcN (Fig. 8*A*). In the presence of insulin, however, GlcN-6-P was detected in the cells with 0.5 mmol/l GlcN (2.26 ± 0.11 nmol/mg protein) and increased by as much as an order of magnitude between 0.5 and 2.5 mmol/l GlcN (Fig. 8*B*; note that the difference in the scale of the ordinates is 40× between Fig. 8*A* and *B*). The dose-dependent increase in GlcN-6-P concentration after preincubation with GlcN in the presence of insulin correlated positively with the observed decrease in acute insulin-stimulated glucose transport ($r = 0.94$, $P < 0.05$, Fig. 8*C*).

PI-3 kinase activity. In an effort to determine if glucose or GlcN-induced insulin resistance was associated with impaired insulin signal transduction, we assayed PI-3 kinase activity as described in CELL CULTURE AND GENERAL METHODS. After acute 5-min maximal insulin stimulation (100 nmol/l), IRS-1–associated PI-3 kinase activity increased ~20-fold. This insulin-induced increase was not significantly affected by preincubation with either GlcN or high glucose in the presence of insulin (Fig. 9), suggesting that if a signaling defect exists, it is distal to PI-3 kinase.

DISCUSSION

Our model of glucose-induced insulin resistance in 3T3-L1 adipocytes is consistent with data from several laboratories, i.e., glucose and insulin act synergistically to downregulate basal and insulin-stimulated glucose transport, and the effect of high glucose is mimicked by GlcN at lower concentrations (Fig. 1). This downregulation is time dependent, requiring several hours. The mechanism, however, is controversial.

In most experiments, we measured 2-DOG uptake as an indicator of glucose transport. The cells were deprived of insulin and FBS for 2 h and then pre-equilibrated for 25 min in glucose-free media before starting the 5-min 2-DOG uptake assay to minimize differences in intracellular concentrations of glucose, glucose-6-P, and GlcN-6-P between treatment groups. Glucose-6-P is a potent inhibitor of hexokinase (28), whereas 2-DOG-6-P (28) and GlcN-6-P (14) are relatively weak inhibitors. Therefore, the decreased acute insulin response of 2-DOG uptake observed in cells that had been preincubated for 18 h with 0.6–0.3 nmol/l insulin in the presence of high glucose or

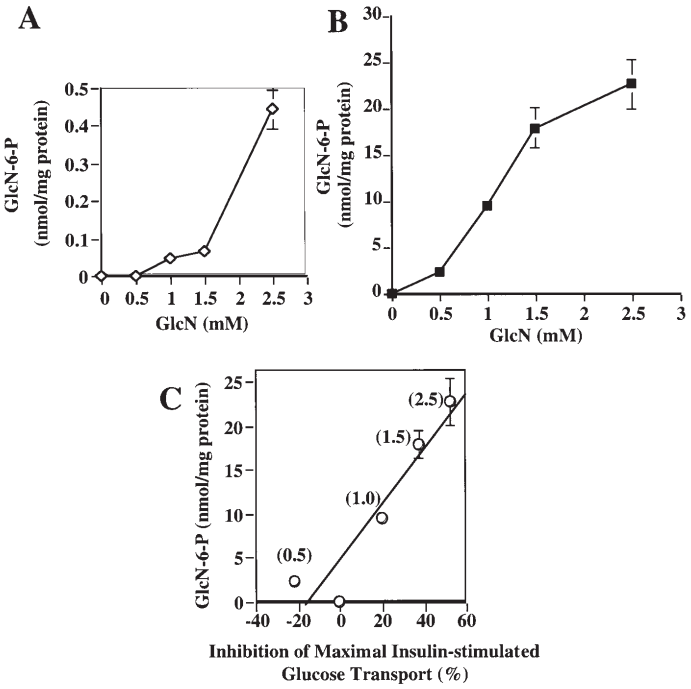

FIG. 8. GlcN-6-P concentration. PCA extracts of 3T3-L1 adipocytes were derivatized with *o*-phthaldialdehyde, and GlcN-6-P was determined fluorometrically by reverse-phase HPLC. Cells were processed after an 18-h preincubation with 5 mmol/l glucose supplemented with increasing concentrations of GlcN (0.1–2.5 mmol/l) in either the absence (*A*) or presence (*B*) of 0.6 nmol/l insulin. Please note the 40-fold scale difference in the *y*-axis between *A* and *B*. *C*: GlcN-6-P levels strongly correlated ($r = 0.938$, $P < 0.05$) with the inhibition of insulin-stimulated glucose transport after preincubation with increasing concentrations of GlcN (0.5–2.5 mmol/l, shown in Fig. 5). Numbers in parentheses indicate GlcN concentrations in the media. Data points represent means ± SE from 3 experiments performed in duplicate.

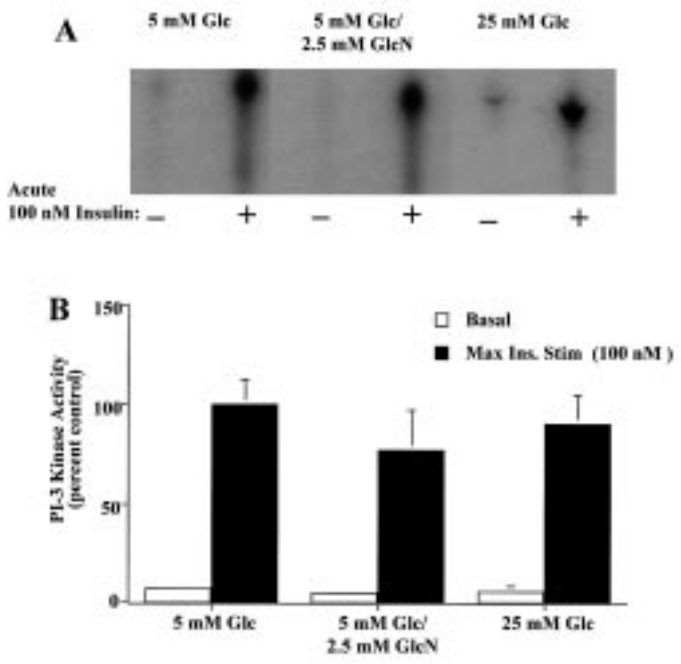

FIG. 9. PI-3 kinase activity. Cells were preincubated with 0.6 nmol/l insulin with either 5 mmol/l glucose (Glc), 5 mmol/l glucose plus 2.5 mmol/l GlcN, or 25 mmol/l glucose. Cells were prepared for acute insulin stimulation as described in the legend of Fig. 1. Total cell extracts were prepared after a 3-min stimulation with or without 100 nmol/l insulin and immunoprecipitated with rabbit α–IRS-1 (2 µg). IRS-1–associated PI-3 kinase activity was assayed. *A*: A representative autoradiogram demonstrating [^{32}P]phosphatidyl inositol-3-phosphate generation after acute stimulation with or without 100 nmol/l insulin. *B*: Data are quantitated as means ± SE from 3 experiments performed in duplicate. In each experiment, data were normalized to the IRS-1–associated PI-3 kinase activity measured in cells preincubated with 5 mmol/l glucose plus 0.6 nmol/l insulin and acutely stimulated with 100 nmol/l insulin.

GlcN likely represents mainly downregulation of transport rather than inhibition of hexokinase activity. This conclusion is supported by the fact that insulin-stimulated 3-OMG transport was inhibited under the same conditions as 2-DOG uptake. The inhibition of the former was slightly less than that of the latter (compare Fig. 1*A* and *C*), which may reflect technical difficulties associated with measuring initial rates of 3-OMG transport, particularly in dish-adherent cells that cannot be as rapidly separated from the medium as cells in suspension. Whereas we cannot rule out the possibility that hexokinase inhibition by glucose-6-P and/or GlcN-6-P contributed to the observed downregulation of 2-DOG uptake, based on the 3-OMG transport data, it was likely a minor contribution.

In our studies, glucose/GlcN-induced glucose transport downregulation occurred without detectable changes in total expression of GLUT4 or GLUT1. Chronic exposure to pharmacological doses of insulin (≥100 nmol/l) have been shown by several laboratories to decrease GLUT4 and increase GLUT1 expression in 3T3-L1 adipocytes (20,29–32). Decreased GLUT4 expression reflects in part insulin-mediated repression of the GLUT4 promoter (33) and in part accelerated degradation of the GLUT4 protein (30). The insulin-mediated stimulation of GLUT1 gene expression appears to be mediated, at least in part, by activation of protein kinase B (PKB)/Akt (34). However, even when using high insulin doses, several laboratories concluded that exposure of 3T3-L1 adipocytes to insulin for 10–24 h caused only mild or no decrease in total GLUT4 expression, which did not account for the marked downregulation of insulin-stimulated glucose transport and GLUT4 translocation (32,35,36). Prolonged exposure to 100–500 nmol/l insulin markedly accelerates the degradation of IRS-1 protein and strongly inhibits the insulin-mediated tyrosine phosphorylation of IRS-1 and activation of PI-3 kinase (32,37). In contrast to the above articles, we used physiological doses of insulin during preincubation, which can occur in plasma postprandially in vivo and are commonly attained in insulin-resistant conditions (4). However, Thomson et al. (20) reported insulin dose-dependent decreased GLUT4 protein expression after exposing 3T3-L1 adipocytes to low insulin concentrations similar to those used here. They proposed that the insulin-mediated desensitization of glucose transport directly reflected decreased GLUT4 expression, which was controlled posttranslationally (i.e., GLUT4 degradation) and required the presence of glucose or GlcN (20). There are several differences in experimental design that may have contributed to the variation in results. The concentration of FBS during preincubation was 10% in the study by Thomson et al. and 1% in our experiments; the media were changed every 2 h in the study by Thomas et al. to maintain glucose and insulin concentrations constant over 12 h, whereas cells were

undisturbed and glucose and insulin in the media were decreasing over 18 h in the experiments reported here. In studies in which cells were exposed to low insulin concentrations (0.05–5 nmol/l) for 12 h, GLUT4 was quantitated in the low-density microsomal (LDM) fraction versus the total cell extracts or unfractionated total membrane preparations in this article. Thus, it is possible that in the study by Thomson et al. (20), GLUT4 was segregated, in part, in a different cellular compartment after chronic insulin treatment. Finally, because 3T3-L1 fibroblasts have been propagated and differentiated in different laboratories for many years, clonal differences may have arisen. The present study demonstrates that marked insulin resistance of glucose transport can develop in cells after pre-exposure to low-dose insulin in the presence of high glucose (but not low glucose) without detectable changes in glucose transporter expression, suggesting the involvement of alternate mechanisms in the development of glucose toxicity.

Insulin's major effect in stimulating glucose transport in responsive cells is the induction of GLUT4 translocation from an LDM-associated intracellular compartment to the cell membrane (3). We were surprised to find that insulin was equally effective in acutely increasing plasma membrane–associated GLUT4 in cells preincubated with or without insulin in the presence of low or high glucose, as assessed by the "lawn assay." Inhibition of insulin-stimulated glucose transport distal to the translocation of GLUT4-containing vesicles (GCV) may reflect impaired fusion of GCV with the cell membrane, inappropriate intercalation, or decreased GLUT4 intrinsic activity. The insulin resistance of glucose transport after stimulation of certain G-protein–coupled receptors may reflect impaired fusion of translocated GCV (38). Although GLUT4 expression is unchanged, muscles overexpressing GLUT1 exhibit markedly increased basal glucose flux and are resistant to insulin stimulation of glucose transport in vitro (39). The translocation and intercalation of GLUT4 into the cell membrane (as assessed by exofacial photo affinity labeling after insulin stimulation) is normal, suggesting that chronically increased glucose flux into the cell impairs the ability of plasma membrane–associated GLUT4 to transport glucose (40). In 3T3-L1 adipocytes, pretreatment with low doses of the PI-3 kinase inhibitor wortmannin downregulated insulin-stimulated glucose transport without affecting GLUT4 translocation or membrane insertion, whereas higher doses inhibited all of the above processes (41). Thus, as in our model of glucose toxicity, activation of glucose transport can be dissociated from GLUT4 translocation. In both 3T3-L1 adipocytes and L-6 myocytes, insulin-mediated activation of p38 MAP kinase may be involved in activating GLUT4 at the cell membrane (21).

Chronic infusion of glucose into rats caused marked insulin resistance without affecting GLUT4 expression or translocation in skeletal muscle (42). The molecular mechanism(s) by which chronically increased glucose flux downregulates glucose transport at step(s) distal to GLUT4 translocation is unknown. Our data indicate that insulin-stimulated PI-3 kinase activation was not inhibited by preincubation in high glucose in the presence of 0.6 nmol/l insulin. However, we cannot rule out the possibility that the subcellular distribution of IRS-1–associated activated PI-3 kinase may have been altered (43). Two recent articles suggest that glucose-induced insulin resistance of glucose transport in muscle occurs at step(s) distal to PI-3 kinase and may involve, at least in part, impaired activation of Akt/PKB (44,45). The complex machinery that regulates docking and fusion of GCV is under intense investigation (46,47) and may include proteins that regulate GLUT4 activity.

In contrast to high glucose, preincubation with GlcN in the presence of insulin did inhibit GLUT4 translocation in response to subsequent acute insulin stimulation. The inhibition was GlcN dose-dependent and was observed at the lowest dose of GlcN (1 mmol/l) that elicited glucose transport insulin resistance in our system. In vivo infusion of GlcN has been reported to inhibit insulin-stimulated GLUT4 translocation in muscle (10). The discrepancy between the effects of high glucose and GlcN in our system was the first indication that the 2 agents may desensitize glucose transport via different mechanisms. The lack of correlation between the accumulation of UDP-HexNAc and the development of insulin-resistant glucose transport further suggested that GlcN may not mimic the effects of high glucose. In the absence of insulin, preincubation with 2.5 mmol/l GlcN increased UDP-HexNAc 4-fold in cells without affecting the acute insulin response of glucose transport. On the other hand, preincubation with high glucose plus insulin increased UDP-HexNAc by only ~30%, but the subsequent insulin response was downregulated to the same extent as after incubation with 2.5 mmol/l GlcN plus insulin, which elevated UDP-HexNAc 9-fold. Furthermore, preincubation with 0.5 mmol/l GlcN plus insulin increased UDP-HexNAc maximally without significantly affecting basal or insulin-stimulated glucose transport. Thus, in a glucose-poor milieu, accumulation of the major HSP products is insufficient for the development of insulin resistance. Because GlcN competes poorly with glucose for transport into muscle cells, it is difficult to assess whether the effects of GlcN and high glucose are additive.

Under physiological conditions, glucose flux via HSP represents a relatively small fraction of total glucose flux, and its entry into the pathway is limited by GFAT activity (7,8). In our experiments, GlcN-6-P accumulation was insulin and GlcN dose-dependent. This result is consistent with insulin accelerating GlcN transport into the cell (7) and suggests that when GlcN enters cells bypassing GFAT, its downstream metabolism is limited at 1 of 2 early steps distal to hexokinase, i.e., acetylation of GlcN-6-P to GlcNAc-6-P or conversion of GlcNAc-6-P to UDP-HexNAc. The marked GlcN dose-dependent decline in UTP concentration suggests that the latter step may be limiting. Accumulation of GlcN-6-P in heart (~700-fold) and to a lesser extent in skeletal muscle (~500-fold) has been recently observed in vivo in rats infused with GlcN during a euglycemic insulin clamp (14). Trapping of high-energy phosphate as GlcN-6-P likely contributed to the decline in ATP observed in cells pre-exposed to GlcN plus insulin, consistent with the data of Hresko et al. (27). The degree of ATP depletion in response to similar GlcN doses was smaller in our model than in the study by Hresko et al. This likely reflects the fact that in the study by Hresko et al., cells were exposed to GlcN in glucose-free media or in the presence of much higher insulin concentrations than those used in our studies; both conditions would markedly enhance GlcN entry into the cells. In the study by Hresko et al., GlcN inhibited the acute insulin response of GLUT4 translocation and insulin-stimulated activation of the insulin receptor, IRS-1, and PI-3 kinase as a consequence of ATP depletion. In contrast, under our

milder experimental conditions, GlcN inhibited insulin-stimulated glucose transport and GLUT4 translocation but not PI-3 kinase activation, consistent with impaired signal transduction distal to PI-3 kinase. In the presence of insulin, we observed GlcN dose-dependent increases in GDP. Although GTP was not quantitated, it likely declined in parallel with ATP during incubation with GlcN. The small GTP binding protein Rab4 is thought to be critical in insulin-stimulated GCV translocation (47,48). A decline in the GTP/GDP ratio may be inhibitory by limiting Rab4 activation.

Our data agree with the major conclusion of Hresko et al. (27), which is GlcN has metabolic effects different from those of high glucose. Both agents induce insulin resistance of glucose transport in 3T3-L1 adipocytes but via different mechanisms. Our data does not infer that products of HSP may not contribute to glucose-induced insulin resistance. Numerous in vivo studies in different models that do not involve GlcN administration show correlations between insulin resistance and enhanced accumulation of UDP-HexNAc in muscle (15–17,49,50). GFAT activity is increased in muscles of genetic rodent models of insulin resistance (16,17) and in muscles of patients with uncontrolled type 2 diabetes (51). Transgenic mice overexpressing GFAT in muscle and fat develop insulin resistance (52,53). 3T3-L1 adipocytes are differentiated from an immortal fibroblast cell line that is chronically maintained in media containing high glucose concentrations (20–25 mmol/l) before and during differentiation. This may cause selection toward cells that are best adapted to this milieu. Although data in 3T3-L1 adipocytes may not be readily extrapolated to other systems, e.g., in vivo studies of skeletal muscle, we feel that investigations using GlcN to model the role of HSP in glucose-induced insulin resistance need to be interpreted with caution.

ACKNOWLEDGMENTS

This work was supported in part by National Institute of Diabetes and Digestive and Kidney Diseases Research Grant DK-02001 (to M.G.B). B.A.N. was supported at different times by a summer student research fellowship and a Medical Scholars Fellowship (both from the American Diabetes Association), a South Carolina Electric and Gas scholarship, and a Medical Scientist Training Grant (GM-08716-01) from the National Institute of General Medical Sciences.

We are grateful to Drs. Morris Birnbaum and Scott Summers for valuable advice in developing the lawn assay; to Dr. Mark Willingham for advice, assistance, and stimulating discussions; and to Mr. James Nicholson for assistance in optimizing immunofluorescence quantitation. We thank Dr. Mike Mueckler for generous gifts of GLUT4 and GLUT1 antibodies and Lilly Research Laboratories for gifts of recombinant crystalline human insulin. We gratefully acknowledge the valuable technical assistance of Jeff A. Koning in the initial characterization of this model and the expert assistance of Ms. Barbara Wojciechowski, MS, with the statistical analyses.

Parts of this work were presented at the 1998 and 1999 Annual Meetings of the American Diabetes Association.

REFERENCES

1. Rossetti L, Giaccari A, Defronzo R: Glucose toxicity. *Diabetes Care* 13:610–630, 1990
2. Yki-Järvinen H, Helve E, Koivisto V: Hyperglycemia decreases glucose uptake in type 1 diabetes. *Diabetes* 36:892–896, 1987
3. Shepherd PR, Kahn BB: Glucose transporters and insulin action: implications for insulin resistance and diabetes mellitus. *N Engl J Med* 341:248–257, 1999
4. Cline GW, Petersen KF, Krssak M, Shen J, Hundal RS, Trajanoski Z, Inzucchi S, Dresner A, Rothman DL, Shulman GI: Impaired glucose transport as a cause of decreased insulin-stimulated muscle glycogen synthesis in type 2 diabetes. *N Engl J Med* 341:240–246, 1999
5. Garvey WT, Olefsky J, Matthaei S, Marshall S: Glucose and insulin co-regulate the glucose transport system in primary cultured adipocytes: a new mechanism of insulin resistance. *J Biol Chem* 262:189–197, 1987
6. Lima F, Thies R, Garvey WT: Glucose and insulin regulate insulin sensitivity in primary cultured adipocytes without affecting insulin receptor kinase activity. *Endocrinology* 128:2415–2426, 1991
7. Marshall S, Bacote V, Traxinger R: Discovery of a metabolic pathway mediating glucose-induced desensitization of the glucose transport system. *J Biol Chem* 266:4706–4712, 1991
8. Robinson KA, Sens D, Buse MG: Pre-exposure to glucosamine induces insulin resistance of glucose transport and glycogen synthesis in isolated rat skeletal muscles: study of mechanisms in muscle and in rat-1 fibroblasts overexpressing the human insulin receptor. *Diabetes* 42:1333–1346, 1993
9. Rossetti L, Hawkins M, Chen W, Gindi J, Barzilai N: In vivo glucosamine infusion induces insulin resistance in normoglycemic but not hyperglycemic conscious rats. *J Clin Invest* 96:132–140, 1995
10. Baron A, Zhu J, Weldon H, Maianu L, Garvey WT: Glucosamine induces insulin resistance in vivo by affecting GLUT4 translocation in skeletal muscle: implications for glucose toxicity. *J Clin Invest* 96:2792–2801, 1995
11. Patti M, Virkamäki A, Landaker E, Kahn CR, Yki-Järvinen H: Activation of the hexosamine pathway by glucosamine in vivo induces insulin resistance of early postreceptor insulin signaling events in skeletal muscle. *Diabetes* 48:1562–1571, 1999
12. Kim Y, Zhu J, Zierath J, Shen H, Baron A, Kahn BB: Glucosamine infusion in rats rapidly impairs insulin stimulation of phosphoinositide 3-kinase but does not alter activation of Akt/protein kinase B in skeletal muscle. *Diabetes* 48:310–320, 1999
13. Chen H, Ing B, Robinson KA, Feagin AC, Buse MG, Quon MJ: Effects of overexpression of glutamine:fructose-6-phosphate amidotransferase (GFAT) and glucosamine treatment on translocation of GLUT4 in rat adipose cells. *Mol Cell Endocrinol* 135:67–77, 1997
14. Virkamäki A, Yki-Järvinen H: Allosteric regulation of glycogen synthase and hexokinase by glucosamine-6-phosphate during glucosamine-induced insulin resistance in skeletal muscle and heart. *Diabetes* 48:1101–1107, 1999
15. Robinson KA, Weinstein M, Lindenmayer G, Buse MG: Effects of diabetes and hyperglycemia on the hexosamine synthesis pathway in rat muscle and liver. *Diabetes* 44:1438–1446, 1995
16. Buse MG, Robinson KA, Gettys T, McMahon E, Gulve E: Increased activity of the hexosamine synthesis pathway in muscles of insulin-resistant *ob/ob* mice. *Am J Physiol* 272:E1080–E1088, 1997
17. Buse MG, Robinson KA, Marshall BA, Mueckler MM: Differential effects of GLUT1 or GLUT4 overexpression on hexosamine biosynthesis by muscles of transgenic mice. *J Biol Chem* 271:23197–23202, 1996
18. Block NE, Menick DR, Robinson KA, Buse MG: Effect of denervation on the expression of two glucose transporter isoforms in rat hindlimb muscle. *J Clin Invest* 88:1546–1552, 1991
19. Frost S, Lane M: Evidence for the involvement of vicinal sulfhydryl groups in insulin-activated hexose transport by 3T3-L1 adipocytes. *J Biol Chem* 260: 2646–2652, 1985
20. Thomson M, Williams M, Frost S: Development of insulin resistance in 3T3-L1 adipocytes. *J Biol Chem* 272:7759–7764, 1997
21. Sweeney G, Somwar R, Ramlal T, Volchuk A, Ueyama A, Klip A: An inhibitor of p38 mitogen-activated protein kinase prevents insulin-stimulated glucose transport but not glucose transporter translocation in 3T3-L1 adipocytes and L6 myotubes. *J Biol Chem* 274:10071–10078, 1999
22. Robinson L, Pang S, Harris D, Heuser J, James DE: Translocation of the glucose transporter (GLUT4) to the cell surface in permeabilized 3T3-L1 adipocytes: effects of ATP, insulin, and GTPγS and localization of GLUT4 to clathrin lattices. *J Cell Biol* 117:1181–1196, 1992
23. Fingar DC, Hausdorff S, Blenis J, Birnbaum MJ: Dissociation of pp70 ribosomal protein S6 kinase from insulin-stimulated glucose transport in 3T3-L1 adipocytes. *J Biol Chem* 268:3005–3008, 1993
24. Kohn A, Summers SA, Birnbaum MJ, Roth RA: Expression of a constitutively active Akt Ser/Thr kinase in 3T3-L1 adipocytes. *J Biol Chem* 271:31372–31378, 1996
25. Wang W, Hansen P, Marshall BA, Holloszy JO, Mueckler MM: Insulin unmasks a COOH-terminal GLUT4 epitope and increases glucose transport across t-tubules in skeletal muscle. *J Cell Biol* 135:415–430, 1996

26. Kelly KL, Ruderman NB, Chen KS: Phosphatidylinositol-3-kinase in isolated rat adipocytes: activation by insulin and subcellular distribution. *J Biol Chem* 267:3423–3428, 1992
27. Hresko R, Heimberg H, Chi M, Mueckler MM: Glucosamine-induced insulin resistance in 3T3-L1 adipocytes is caused by depletion of intracellular ATP. *J Biol Chem* 273:20658–20668, 1998
28. Hansen PA, Gulve EA, Holloszy JO: Suitability of 2-deoxyglucose for in vitro measurement of glucose transport activity in skeletal muscle. *J Appl Physiol* 76:979–985, 1994
29. Clancy BM, Czech MP: Hexose transport stimulation and membrane redistribution of glucose transporter isoforms in response to cholera toxin, dibutryl cyclic AMP, and insulin in 3T3-L1 adipocytes. *J Biol Chem* 265:12434–12443, 1990
30. Sargeant RJ, Pâquet MR: Effect of insulin on the rates of synthesis and degradation of GLUT1 and GLUT4 glucose transporters in 3T3-L1 adipocytes. *Biochem J* 290:913–919, 1993
31. Flores-Riveros JR, McLenithan JC, Ezaki O, Lane MD: Insulin down-regulates expression of the insulin-responsive glucose transporter (GLUT4) gene: effects on transcription and mRNA turnover. *Proc Natl Acad Sci U S A* 90:512–516, 1993
32. Ricort JM, Tanti J-F, Van Oberghen E, LeMarchand-Brustel Y: Alterations in insulin signalling pathway induced by prolonged insulin treatment in 3T3-L1 adipocytes. *Diabetologia* 38:1148–1156, 1995
33. Cooke DW, Lane MD: The transcription factor nuclear factor I mediates repression of the GLUT4 promoter by insulin. *J Biol Chem* 274:12917–12924, 1999
34. Barthel A, Okino ST, Liao J, Nakatani K, Li J, Whitlock JP, Roth RA: Regulation of GLUT1 gene transcription by the serine/threonine kinase Akt1. *J Biol Chem* 274:20281–20286, 1999
35. Tordjman KM, Leingang KA, James DE, Mueckler MM: Differential regulation of two distinct glucose transporter species in 3T3-L1 adipocytes: effect of chronic insulin and tolbutamide treatment. *Proc Natl Acad Sci U S A* 86:7761–7765, 1989
36. Kozka IJ, Clark AE, Holman GD: Chronic treatment with insulin selectively down-regulates cell surface GLUT4 glucose transporters in 3T3-L1 adipocytes. *J Biol Chem* 266:11726–11731, 1991
37. Rice KM, Lienhard GE, Garner CW: Regulation of the expression of pp160, a putative insulin receptor signal protein by insulin, dexamethasone, and 1-methyl-3-isobutyl xanthine in 3T3-L1 adipocytes. *J Biol Chem* 267:10160–10167, 1992
38. Vanucci S, Nishimura H, Satoh S, Cushman SW, Holman GD, Simpson IA: Cell accessibility of GLUT4 glucose transporters in insulin stimulated rat adipose cells: modulation by isoprenaline and adenosine. *Biochem J* 288:325–330, 1992
39. Gulve EA, Ren J-M, Marshall BA, Gao J, Hansen PA, Holloszy JO, Mueckler MM: Glucose transport activity in skeletal muscle of mice overexpressing GLUT1: increased basal transport is associated with a defective response to diverse stimuli that activate GLUT4. *J Biol Chem* 269:18366–18370, 1994
40. Hansen PA, Wang W, Marshall BA, Holloszy JO, Mueckler MM: Dissociation of GLUT4 translocation and insulin-stimulated glucose transport in transgenic mice overexpressing GLUT1 in skeletal muscle. *J Biol Chem* 273:18173–18179, 1998
41. Hausdorff SF, Fingar DC, Morioka K, Garza LA, Whiteman EL, Summers SA, Birnbaum MJ: Identification of wortmannin-sensitive targets in 3T3-L1 adipocytes: dissociation of insulin-stimulated glucose uptake and GLUT4 translocation. *J Biol Chem* 274:24677–24684, 1999
42. Davidson MB, Bouch C, Venkatesan N, Karjala RG: Impaired glucose transport in skeletal muscle but normal GLUT4 tissue distribution in glucose infused rats. *Am J Physiol* 267:E808–E813, 1994
43. Czech MP, Corvera S: Signalling mechanisms that regulate glucose transport. *J Biol Chem* 274:1865–1868, 1999
44. Song XM, Kawano Y, Krook A, Ryder JW, Efendic S, Roth RA, Wallberg-Henriksson H, Zierath JR: Muscle fiber type-specific defects in insulin signal transduction to glucose transport in diabetic GK rats. *Diabetes* 48:664–670, 1999
45. Kurowski TG, Lin Y, Luo Z, Tsichlis PN, Buse MG, Heydrick SJ, Ruderman NB: Hyperglycemia inhibits insulin activation of Akt/protein kinase B but not phosphatidylinositol 3-kinase in rat skeletal muscle. *Diabetes* 48:658–663, 1999
46. Rea S, James DE: Moving GLUT4: the biogenesis and trafficking of GLUT4 storage vesicles. *Diabetes* 46:1667–1677, 1997
47. Pessin JE, Thurmond DC, Elmendorf JS, Coker KJ, Okada S: Molecular basis of insulin-stimulated GLUT4 vesicle trafficking. Location! Location! Location! *J Biol Chem* 274:2593–2596, 1999
48. Cormont M, Bortoluzzi MN, Gautier N, Mari M, Van Oberghen E, LeMarchand-Brustel Y: Potential role of Rab4 in the regulation of subcellular localization of GLUT4 at the cell surface. *Mol Cell Biol* 16:6879–6886, 1996
49. Hawkins M, Angelov I, Liu R, Barzilai N, Rossetti L: The tissue concentration of UDP-N-acetylglucosamine modulated the stimulatory effect of insulin on skeletal muscle glucose uptake. *J Biol Chem* 272:4889–4895, 1997
50. Hawkins M, Barzilai N, Lui R, Hu M, Chen W, Rossetti L: Role of the glucosamine pathway in fat-induced insulin resistance. *J Clin Invest* 99:2173–2182, 1997
51. Yki-Järvinen H, Daniels M, Virkamäki A, Mäkimattila S, DeFronzo R, McClain D: Increased glutamine:fructose-6-phosphate amidotransferase activity in skeletal muscle of patients with NIDDM. *Diabetes* 45:302–307, 1996
52. Hebert LF, Daniels M, Zhou J, Crook E, Simmons S, Neidigh J, Baron A, McClain D: Overexpression of glutamine-fructose-6-phosphate amidotransferase in transgenic mice leads to insulin resistance. *J Clin Invest* 98:930–936, 1996
53. Cooksey RC, Hebert LF, Zhu J-H, Wofford P, Garvey WT, McClain DA: Mechanism of hexosamine-induced insulin resistance in transgenic mice overexpressing glutamine:fructose-6-phosphate amidotransferase: decreased glucose transporter GLUT4 translocation and reversal by treatment with thiazolidinedione. *Endocrinology* 140:1151–1157, 1999